

Seismic swarms, fluid flow and hydraulic conductivity in the forearc offshore North Costa Rica and Nicaragua

Martin Thorwart · Yvonne Dzierma ·
Wolfgang Rabbel · Christian Hensen

Received: 20 September 2012 / Accepted: 1 September 2013 / Published online: 10 October 2013
© Springer-Verlag Berlin Heidelberg 2013

Abstract At the continental margin of north Costa Rica and Nicaragua, the strongly hydrated Cocos Plate subducts beneath the Caribbean Plate. From the downgoing Cocos plate fluids are released through extensional fractures in the overriding plate. At the seafloor, they form fluid seeps, mounds and other types of fluid expulsion. Using an offshore temporary seismic network, we investigated seismicity possibly related to these processes and observed several swarms of earthquakes located on the continental slope trenchward of the seismogenic zone of S Nicaragua. The seismicity occurred within the downgoing plate, near the plate interface and in the overriding plate. We interpret these swarm events as an expression of pore pressure propagation under critical stress conditions driven by fluid release from the downgoing plate. In order to estimate hydraulic diffusivity and permeability values, we applied a theory developed for injection test interpretation to the spatio-temporal development of the swarms. The resulting diffusivity and permeability values are in the ranges of 28–305 m²/s and 3.2×10^{-14} m²– 35.1×10^{-14} m², respectively, applying to the continental and oceanic crust near the plate interface. These values are somewhat larger than observed in drill logs on the margin wedge off north Costa Rica, but of comparable magnitude to values estimated for the Antofagasta 1995 earthquake aftershock sequence.

Keywords Central American subduction zone · Earthquake swarms · Diffusivity · Permeability

Introduction

Along the world's convergent margins, fluids are continually recycled from the ocean floor into the crust and upper mantle and back to the Earth's surface and interior. Water and other volatiles are carried into the subduction zone with the downgoing plate by sediments and hydrated oceanic crust and mantle. They are released at different depth and along different pathways along which the presence of fluids causes a variety of processes, from shallow seeps providing home to chemosynthetic life forms to the position and extent of the seismogenic zone and volcanic arc (Ranero et al. 2008; Rüpke et al. 2004).

Offshore north Costa Rica and Nicaragua, the strongly hydrated Cocos Plate subducts beneath the Caribbean Plate along the erosional Central American margin (deMets et al. 1994; Ranero and von Huene 2000; Vannucchi et al. 2001, 2003). Unlike in accretionary margins, where fluids released by dehydration reactions under the continental slope typically migrate upwards along the décollement and major splay faults, fluid release at erosional margins seems to occur through numerous fractures in the overriding plate driven by extensional tectonics (Ranero et al. 2008). Fluid seeps in this region have been observed at abundant seafloor mounds and other types of fluid expulsion; typically, they appear as sidescan sonar backscatter anomalies and are identified by the presence of chemosynthetic communities and by characteristic chemical anomalies in the pore water (Bohrmann et al. 2002; Hensen et al. 2004, 2007; Sahling et al. 2008; Klauke et al. 2008; Karaca et al. 2010). In characterizing the dynamics of fluid transport, these approaches have suffered from the fact

M. Thorwart (✉) · Y. Dzierma · W. Rabbel
SFB 574, Department of Geophysics, Institute of Geosciences,
Christian-Albrechts-Universität, Otto-Hahn-Platz 1, 24118 Kiel,
Germany
e-mail: thorwart@geophysik.uni-kiel.de

C. Hensen
SFB 574, GEOMAR Helmholtz-Zentrum für Ozeanforschung
Kiel, Wischhofstrasse 1-3, 24148 Kiel, Germany

that most mounds are only intermittently active, and some indicators such as authigenic carbonates cannot tell whether a seep is still active. Others, like geochemical anomalies and flux calculations, provide a measure for the current state of activity, but cannot be used for long-term prediction. It is well known from laboratory and field observations that pore pressure variations play a crucial role in triggering earthquakes. Micro-seismic swarms caused by fluid injection into boreholes have been used to monitor the propagating pore pressure front (Shapiro et al. 1997, 1999, 2002; Shapiro 2000). Here, we present data from a temporary seismic network in order to propose that natural small magnitude earthquake swarms can also be monitored as a complementary technique for investigating fluid migration processes.

This approach offers the opportunity to characterize the spatio-temporal migration of pore pressure on a quantitative basis. In fact, the determination of hydraulic conductivity is an important and extremely difficult task of geophysics (Shapiro 2000), which has only rarely been carried out in the natural environment, undisturbed by drilling or active fluid injection experiments. Therefore, the seismic swarms observed offshore Costa Rica and Nicaragua present a unique possibility to learn about the pore pressure diffusion in this region and estimate critical parameters such as hydraulic diffusivities and permeabilities. In addition to giving insight into the seismicity process, this is of high interest also for ocean drilling projects such as the ongoing IODP deep-sea drilling project “CRISP” (Ranero et al. 2007; Vannucchi et al. 2010).

Hydro-tectonic setting

Fluid flow at the erosional Central American margin

Offshore north Costa Rica and Nicaragua the Cocos Plate subducts beneath the Caribbean Plate along the erosional Middle America Trench (deMets et al. 1994; Fig. 1). In addition to pore fluids in the subducting sediments and crust, the incoming plate carries a large amount of mineral-bound water. On the one hand, this is water carried by abundant smectites and opal in the hemipelagic section of the subducting sediments (Spinelli and Underwood 2004), on the other hand, bending-related faulting provides pathways for sea water to enter the slab and hydrate the slab crust and mantle before entering the trench (von Huene et al. 2000; Ranero et al. 2005; Grevemeyer et al. 2007; Ivandic et al. 2008).

Over the past years, the following scenario for fluid migration pathways in non-accretionary subduction zones has emerged (Fig. 2; Hensen et al. 2004; Ranero et al. 2008; Saffer and Tobin 2011): a small frontal prism is followed by a back stop presenting an extension of onshore geology.

Elevated pore fluid pressure in the frontal prism reduces the décollement friction, so that nearly the complete trench sediments can be subducted. Under the slope, fluids released from the subducted plate hydro-fracture the overriding plate, eroding it at its base and migrating upwards through extensional faults to be released at ocean floor vents. Some are also channelled towards the back stop of the sedimentary prism.

Dehydration reactions are strongest under the mid-forearc, where temperatures of 60–120 °C cause the transition from smectite to illite, most likely the largest source of dehydration water at shallow depths of subduction. Below, fluid release ceases corresponding to the onset of the seismogenic zone (Hyndman et al. 1997; Oleskevich et al. 1999). Oceanic crust and mantle dehydration processes mainly occur below the mantle wedge at much higher temperature and pressure conditions (e.g. Rüpke et al. 2002), which is not within the scope of this study.

Mud volcanoes and diapirs at the Costa Rican/Nicaraguan margin

On the middle slope of the continental margin offshore north Costa Rica and Nicaragua, a large density of mud diapirs, mud volcanoes and other fluid emanation sites is observed at water depths of ca. 1,000–2,500 m (Kahn et al. 1996; Bohrmann et al. 2002; Mau et al. 2006; Talukder et al. 2007; Sahling et al. 2008; Petersen et al. 2009). Among the mounds, Mound Culebra is one of the largest, reaching an elevation over 100 m and an area of more than 1 km². Most mounds are cone-shaped features with typical elevations of 10–100 m and 100–1,000 m width (Soeding et al. 2003; Sahling et al. 2008). Many of the mounds are characterized by the presence of authigenic carbonates and chemosynthetic communities (Han et al. 2004; Sahling et al. 2008) fed by active seepage of methane-rich fluids released at greater depth (Hensen et al. 2004; Schmidt et al. 2005; Karaca et al. 2010).

High-resolution seismic studies of the shallow subsurface at Mound Culebra showed that reflectors beneath the mound flanks are bending upwards, then terminate, leaving the mound interior largely free of reflections. This was interpreted as a disruption of the geological structures due to fluid and gas ascent, an interpretation which is supported by elevated heat flow values indicative of fluid advection (Moerz et al. 2005; Fekete 2006).

Data and method

Seismological data

In the framework of the SFB 574 project on “Volatiles and Fluids in Subduction Zones”, 20 ocean bottom

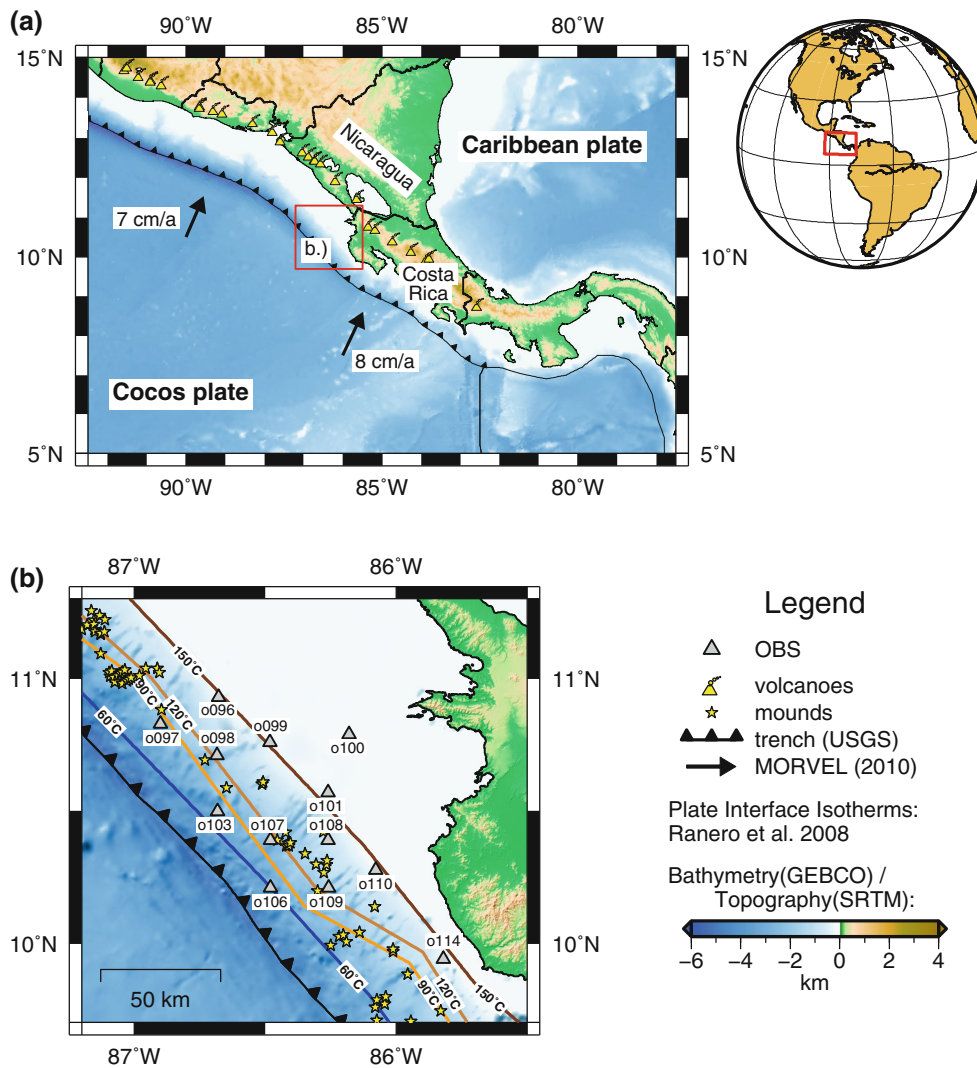
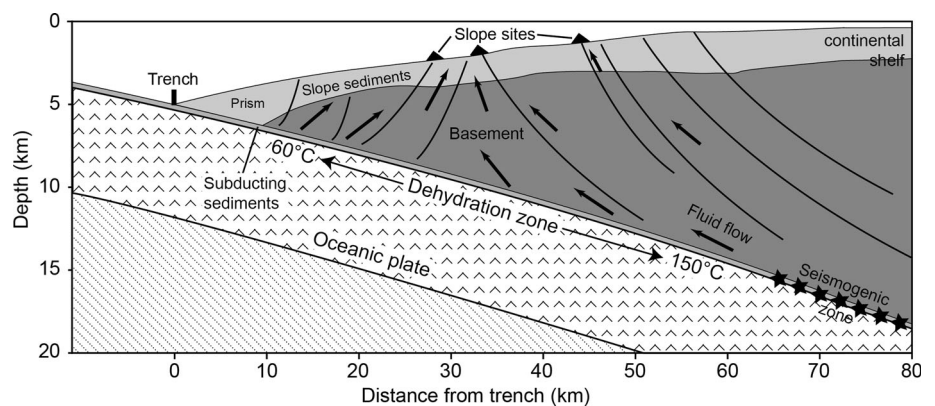


Fig. 1 Location map: **a** Central America subduction zone; the *Cocos Plate* subducts below the *Caribbean Plate*. **b** Investigation area offshore Nicaragua. *Grey triangle*: ocean bottom seismometer station,

yellow star: vent site (Sahling et al. 2008), *coloured line*: isotherms on the plate interface (Ranero et al. 2008)

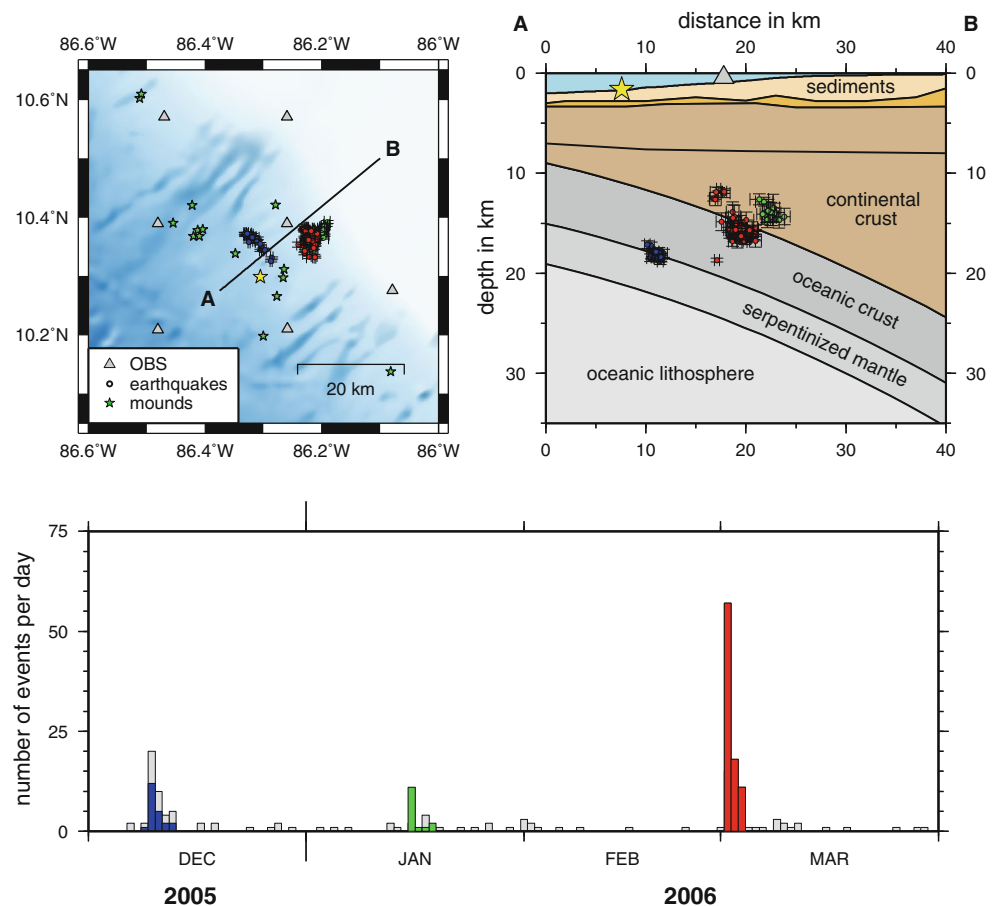
Fig. 2 Hydro-tectonic elements of the shallow part of the subduction zone offshore S Nicaragua. On top of the subducting plate water gets released from the sediments. Fluids can flow along faults in the overriding plate towards the active slope sites. At a temperature of 150 °C most of the sediments are dehydrated. This marks the beginning of the seismogenic zone



seismic stations were deployed offshore north Costa Rica and south Nicaragua from December 2005 to June 2006, half of which were equipped with short-period

seismometers (4.5 Hz) in addition to the hydro-phones. The networks and data quality are presented in detail by Dinc et al. (2011). We use data from 13 ocean bottom

Fig. 3 Seismic swarms near mound Culebra. *Top:* map view of the seismic swarm activity near mound Culebra (*big yellow star*) and depth section along profile AB with projected hypocenters. Earthquakes of 3 swarms took place in December 2005 (*blue circles*), January 2006 (*green circles*) and March 2006 (*red circles*). Ocean bottom seismometer o108 is located directly above the swarms (*grey triangle*). *Bottom:* Temporal evolution of the local seismicity near mount Culebra. The swarms are marked in blue, green and red, respectively



stations with good timing accuracy and data quality (Fig. 1).

The continuous data recordings were searched for earthquake signals by an automatic STA/LTA algorithm followed by a network trigger. The events were then manually picked for analysis and localized using the seismic velocity model of Berhorst (2006).

Several swarms of earthquakes appear to be present in the data set. Three episodes of swarm activity occurred near mound Culebra in December 2005, January 2006 and March 2006, lasting 3–5 days each (Fig. 3). We use the HypoDD routine (Waldhauser and Ellsworth 2000; Waldhauser 2001) to distinguish different swarms and improve the relative location of the events in the swarms. For the localisation, we rely on the relative onset times that could be determined with high accuracy because the events show highly coherent waveforms (Fig. 5). The relative locations obtained by this algorithm proved to be very stable; absolute location, however, is less well constrained. Still, the depth can be estimated from the fact that we observe a travel time difference between the *P*- and *S*-wave onsets of about 4 s at the station o108, directly above the swarms. Assuming an average *P*-wave velocity of 3.5 km/s for the continental slope (Berhorst

2006) and a V_p/V_s ratio of 1.8 (Dinc et al. 2011), we obtained a hypocentral depth of about 15–19 km. The events hence occurred near the plate interface which is located at ca. 15 km depth in this region.

The magnitude of the events could not be directly calculated from these records. Fortunately, five events listed in ISC online bulletin (2011) were recorded independently by Nicaraguan and Costa Rican land stations. From these events, only the $ML = 3.0$ event on 10 December 2005 presented readable signal (not clipped) in OBS o108. Using this event as reference, the relative amplitude ratio could be used to estimate the magnitude of the other events.

Hydraulic model

In the theory relating pore pressure propagation caused by hydraulic tests with induced micro-seismicity it is generally assumed that the crust is in a near-critical state of stress, where a small increase in pore pressure will create clouds of micro-seismicity due to the changes in effective normal stress and friction coefficients (Shapiro et al. 1997, 1999, 2002, 2003). The migration of the pore pressure perturbation p with time t in the rock is governed by the diffusion equation

$$\frac{\partial p}{\partial t} = D \nabla^2 p \quad (1)$$

(Biot 1962; Shapiro et al. 1997), where the hydraulic diffusivity D is given by

$$D = \frac{Nk}{\eta} \quad (2)$$

Here, k denotes the permeability, η the dynamic viscosity of the pore fluid and N the poroelastic modulus depending on the elastic moduli (bulk moduli K and shear moduli μ) of the whole rock (with porosity φ), of the grains and fluid (indexed correspondingly). Index “dry” denotes the corresponding properties of porous rock without pore fill:

$$N = \frac{MP_{\text{dry}}}{H}, \quad (3)$$

$$\alpha = 1 - \frac{K_{\text{dry}}}{K_{\text{grain}}}, \quad (4)$$

$$M = \left(\frac{\varphi}{K_{\text{fluid}}} + \frac{\alpha - \varphi}{K_{\text{grain}}} \right)^{-1}, \quad (5)$$

$$H = P_{\text{dry}} + \alpha^2 M \quad (6)$$

and

$$P_{\text{dry}} = K_{\text{dry}} + \frac{4}{3} \mu_{\text{dry}}. \quad (7)$$

P_{dry} is the P -wave modulus for a dry rock, H is the P -wave modulus of the grains, M is the average bulk modulus of a wet rock, α is the relative difference between the bulk modulus of the grains and the dry rock, this leads to:

$$k = \left(\frac{1}{M} + \frac{\alpha^2}{P_{\text{dry}}} \right) \times \eta \times D \quad (8)$$

An initial perturbation pulse in pore pressure will spread out, producing a growing cloud of events. The time dependent radius $r(t)$ of the propagation front $r(t)$ can be approximated by the relationship

$$r(t) = \sqrt{4\pi Dt} \quad (9)$$

valid for the case of an isotropic medium (Shapiro et al. 1997). The r - t -relation observed from the spreading seismicity cloud can be used to determine the diffusivity and to estimate the permeability of the medium.

While this approach is generally used in the context of fluid injection experiments at boreholes, Shapiro et al. (2003) applied the same parameterisation to the aftershock sequence of the 1995 Antofagasta earthquake and found a spatio-temporal behaviour consistent with fluid triggering. Along the same line of thought, we use this approach for the observed seismic swarms.

Following the interpretation by Shapiro et al. (2003), we consider seismic swarms as starting from an injection or

nucleation point. From the nucleation point, a pore pressure perturbation cloud is supposed to spread out in radial direction, triggering earthquakes near to the propagation front, but also within the affected volume.

For each event in a swarm, the distance and the time of each event relative to the nucleation point can be calculated and plotted. The envelope of all data points in the distance-time diagram shows the temporal evolution of the propagation front of the pressure perturbation, which can be approximated by a parabolic shape (Eq. 9). In a log-log diagram, a straight line with a slope of 0.5 corresponds to a constant diffusivity D . In a first approach, we used the hypocenter of the first event in a swarm as the nucleation point. Times and distances relative to this first event were calculated and plotted in a log-log diagram. Lately, a grid search around the hypocenter of the first event was performed to find a nucleation point for which the envelope of the data points corresponds to a line of constant diffusivity D . For estimating the diffusivity, we determined the envelope lines below which 75, 90 and 98 % of the events fall considering the 75 % envelope as a minimum estimate, the 90 % envelope as the mean value and the 98 % envelope as a maximum estimate of the diffusivity.

Results

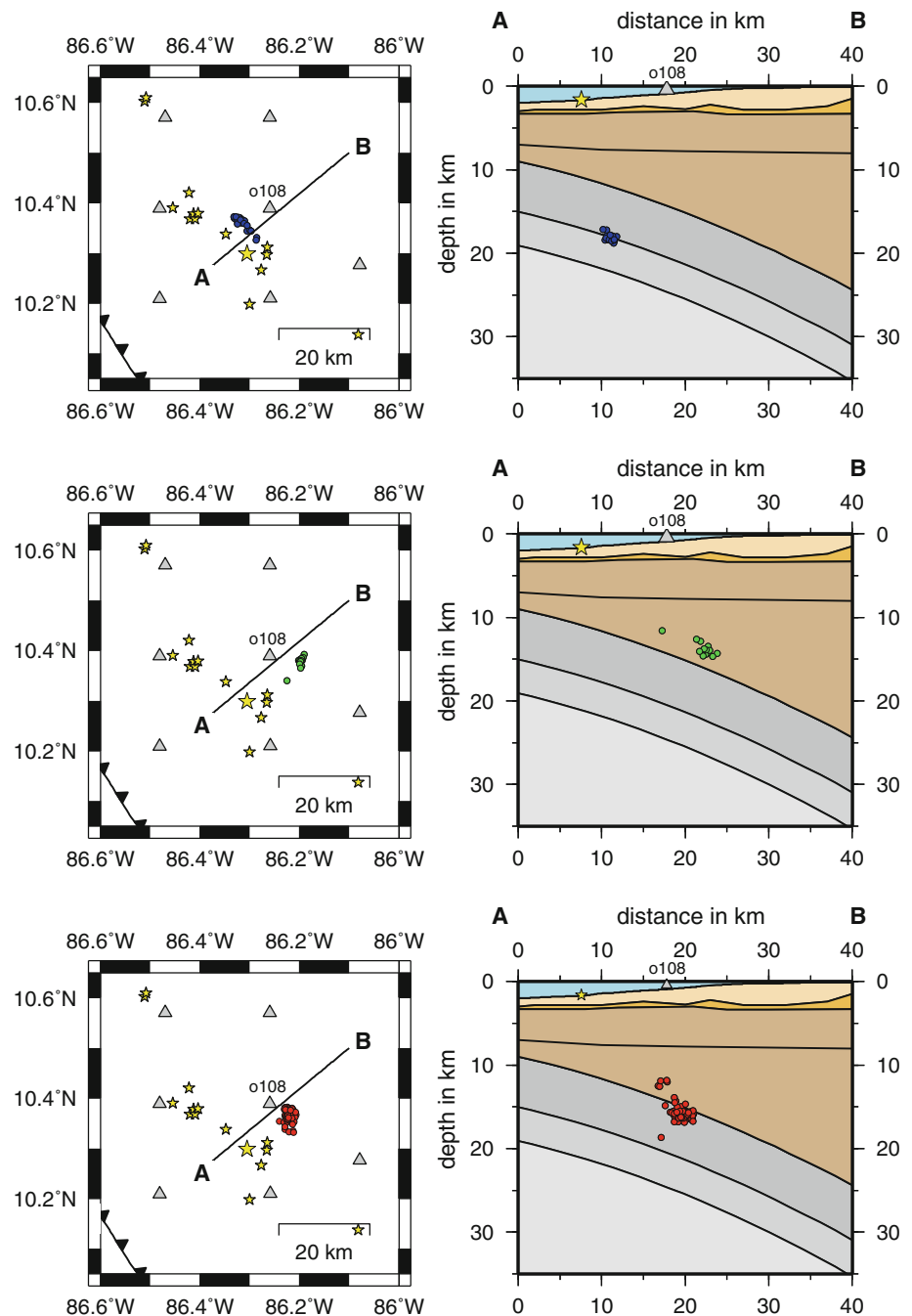
Swarms near Mound Culebra

The identification of swarms in our earthquake catalogue is performed on the grounds of continuous activity and spatial proximity. Three swarms occurred near mound Culebra between December 2005 and March 2006 (Fig. 3) showing seismicity rates up to 70 events per day. Between the swarms, the seismicity rate is less than 5 events per day.

December 2005 swarm

The swarm started in the final hour of December 9th and lasted until December 13th. It consists of 25 earthquakes including three earthquakes on December 10th with a local magnitude ML of 3.4, 3.0 and 3.3, respectively (ISC Online Bulletin 2011). The magnitude of the other events ranges from 1.5 to 3.0. They form a spatial cluster in the down-going slab near to the oceanic Moho with hypocentral depths of about 18 km (Fig. 4, top). The cluster has a linear, trench parallel shape. Its horizontal extent is about 8 km. The location of the earthquakes propagates with time from the northwest to southeast. The P -waveforms of station o108 located directly above the swarm are highly coherent indicating a uniform mechanism for all earthquakes (Fig. 5). This possibly suggests that a bending-related fault had been activated during the swarm.

Fig. 4 Detailed view of seismic swarms at mound Culebra (colour coded as in Fig. 3). *Top to bottom*: map views and depth profiles of December 2005, January 2006 and March 2006 swarms



January 2006 swarm

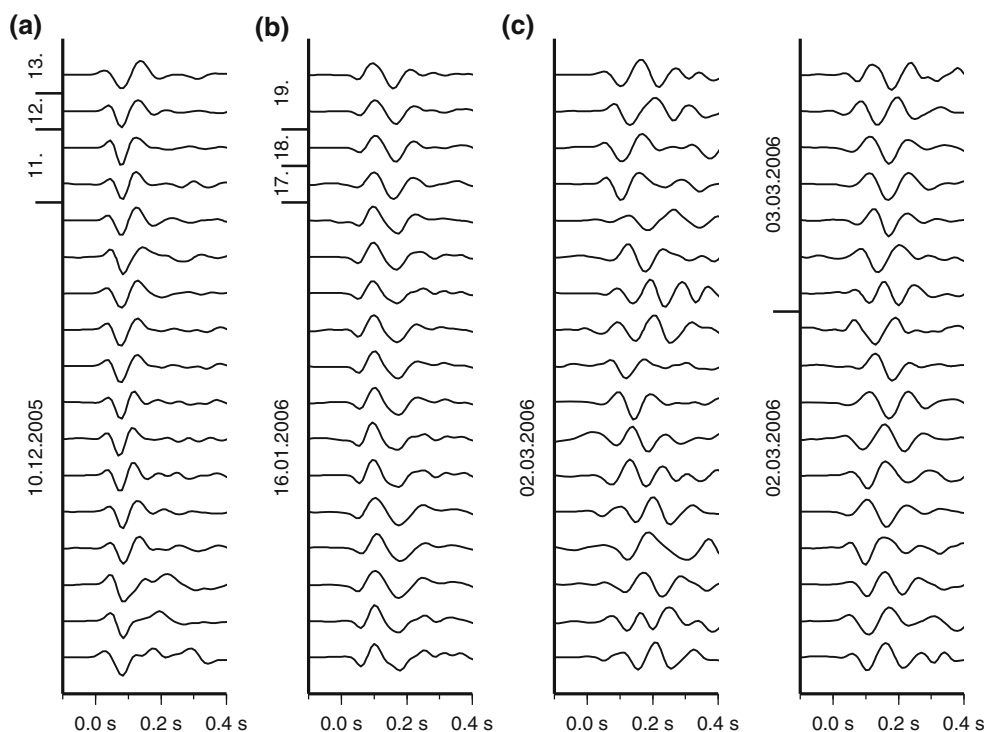
This swarm occurred between 16 and 19 January 2006 with the main activity on 16 January 2006. With 18 events it is the smallest swarm and its magnitudes range from 1.0 to 2.0. The events form a cluster in the overriding plate between the depth of 12 and 15 km (Fig. 4, middle). Due to the size of the earthquakes only few onset times were available and the location errors are bigger than for the other two swarms. There is no distinct trend in the temporal evolution of the cluster. The *P*-

waveforms are again highly coherent, possibly indicating an activation of a fault.

March 2006 swarm

This swarm is the most populated one we analysed in this study. While it lasted only 3 days (from 2 to 4 March 2006), it included a total of 84 events (Fig. 4, bottom). The magnitude of the events ranges from 1.0 to 3.9. Two earthquakes had a local magnitude *ML* of 3.9 and 3.6 (ISC Online Bulletin 2011). The swarm occurred near the plate

Fig. 5 Waveforms of direct *P*-wave arrivals of selected swarm earthquakes. **a** December 2005 swarm. **b** January 2006 swarm. **c** March 2006 swarm. Waveforms are ordered by their occurrence (*bottom to top*) and artificial aligned, respectively, to their *onset*. Swarms **(a)** and **(b)** show similar waveforms for all events indicating a similar fault mechanism. Swarm **(c)** seems to consist of earthquake with several different fault mechanism



interface at a depth of 16 km. It has no distinct form and it extends 3 km north–south, 2 km east–west and 3 km in the vertical direction. No temporal trend can be recognized. It shows incoherent waveforms possibly indicating either the activation of several faults or a complex stress system.

Diffusivity and permeability estimate

The diffusivity estimates for the swarms observed at Mound Culebra (Fig. 6a, b) range from 28 to 921 m²/s corresponding to the 75 and 98 % event envelopes; as an intermediate “best fit” value (corresponding to the 90 % envelope), we obtained a diffusivity of 60 m²/s.

To calculate the permeability from these values, we make the commonly applied assumption that the poro-elastic modulus of low-porosity crystalline rocks can be approximated by the simplified relation:

$$M \approx \left(\frac{\varphi}{K_{\text{fluid}}} + \frac{\alpha}{K_{\text{grain}}} \right)^{-1} \tag{10}$$

The depth of the earthquakes is taken to be approximately 15 km, the temperature is ca. 120 °C. It is known from active seismic experiments (Walther et al. 2000; Berhorst 2006) that the events are placed in a part of the margin wedge presumably formed by a subducted oceanic plateau, more precisely, within the upper effusive crust. Walther et al. (2000) observe a seismic velocity of $V_p = 5.9$ km/s and model a density of 2.9 kg/l. V_s is not precisely known, we calculate it from V_p using a velocity ratio of 1.8. This is

actually somewhat higher than the usually assumed value of 1.73 for average crustal rocks, but indications for fluid presence have been observed both in active seismic (Ivandic et al. 2008) and local earthquake tomography (Dinc et al. 2011), where V_p/V_s of the order of 1.8 and even higher was found. For these values, we obtain an estimate for K_{dry} from the formula

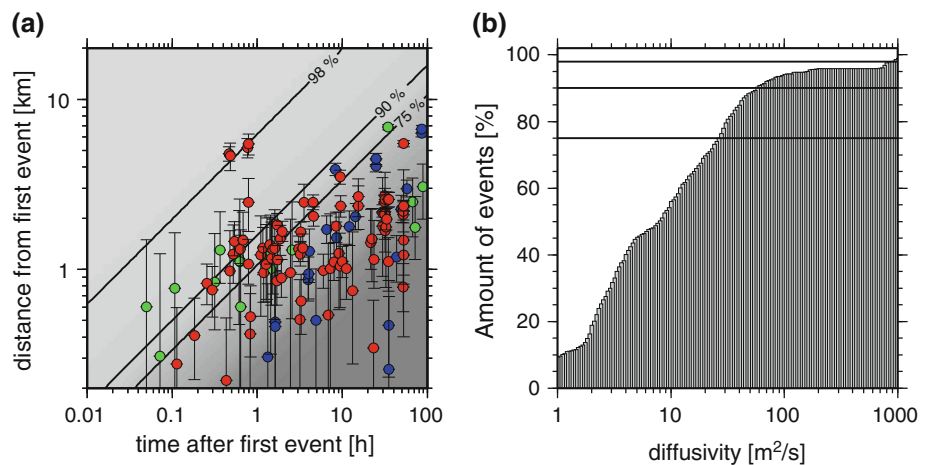
$$K_{\text{dry}} \approx K = \rho \cdot \left(v_p^2 - \frac{4}{3} v_s^2 \right) = \rho \cdot v_p^2 \cdot \left(1 - \frac{4}{3(v_p/v_s)^2} \right) \tag{11}$$

giving a value K_{dry} of 59 GPa. The property K_{grain} can be estimated from literature values for basalt at about 15 km depth (ca. 300 MPa) and 100 °C ($V_p = 6.1$ – 6.6 km/s, $\rho = 2.95$ – 2.98 kg/l, $V_p/V_s = 1.73$ – 1.75 , see e.g. Gebrande 1982). Basalt was chosen because the lithological unit where the swarms are found corresponds probably to the effusive crust of a subducted oceanic plateau (Walther et al. 2000). With the above formula, we obtain $K_{\text{grain}} = 61$ – 72 GPa, and $\alpha = 0.0328$ – 0.181 . We assume a porosity φ of ca. 1 % (range 0.5–1.5 %). For the bulk modulus and dynamic viscosity of water at 300 MPa and 100 °C, we used the values of the International Association for the Properties of Water and Steam (<http://www.iapws.org>, IAPWS Release 2008), $K_{\text{fluid}} = \rho V_p^2 = 4.3$ GPa, $\eta = 0.2897$ mPa s.

With these estimates, we obtain values for M and P_{dry} of 258 and 100 GPa, respectively, and the following relationship between the permeability k and the diffusivity D :

Fig. 6 Estimation of hydraulic diffusivity based on Eq. (9).

a Log–log diagram of time difference and distance relative to the first event of the swarm. Lines of constant diffusivity bounding 75, 90 and 98 % of events are indicated by *solid lines*. **b** Cumulative histogram of events for increasing diffusivity values. 75, 90 and 98 % levels indicated by *solid horizontal lines* correspond to the estimates of *lower bound*, *intermediate value* and *upper bound* of diffusivity



$$k \approx 1.15 \times 10^{-15} \text{ s}^{-1} \times D. \quad (12)$$

Using the diffusivity D values estimated from our seismicity observations, we obtain a permeability of $k = 6.9 \times 10^{-14} \text{ m}^2 = 69 \text{ mD}$ corresponding to the 90 % envelope and a range of $k = 3.2 \times 10^{-14} \text{ m}^2$ – $106.0 \times 10^{-14} \text{ m}^2 = 32$ – 1060 mD corresponding to the 75 and 98 % envelopes.

Discussion

Relationship of seismic swarms with fluid flow

We have until now assumed that the observed seismicity is related with fluids or pore pressure propagating through the fault zones of the forearc, which is the most intuitive interpretation given the alignment near to active vent structures on the continental slope. However, we must consider that alternative explanations may exist, which we will discuss in the following.

Firstly, it may be argued that we are possibly imaging just the seismogenic zone. If this was the case, the question would be difficult to answer why the events are clustered in swarms of recurrent activity. Moreover, temperature profiles across the continental slope and seismicity observed at Nicoya Peninsula (DeShon et al. 2006) suggest that the seismogenic zone is encountered further landward than the observed seismic swarms. All swarms are found approximately between the 120 and 150 °C temperature isolines (Fig. 1). If we assume the onset of seismogenic behaviour to coincide with the 150° temperature contour (as suggested by Ranero et al. 2008), this places the seismic swarms trenchward of the seismogenic zone.

Recurrent rupturing of this part of the plate may be explained by patches of activity related, for example, to subducting topography such as seamounts. A subducting seamount might crack the overriding plate and thus produce a patch of increased seismicity. This explanation does

not apply to the December 2005 and January 2006 swarms because they are located too far below and above the plate interface. But it cannot be excluded for the March 2006 swarm which locates close to the plate interface. A decision cannot be based on seismicity alone, and unfortunately none of the available reflection seismic profiles cuts through the swarms to determine the topography of the plate interface. However, if a subducting seamount cracked the overriding plate, this would be expected to produce spatial clustering in the seismicity, but not the temporal clustering. We would rather expect continuous activity, different from the observed swarm behaviour.

Finally, we know from the work cited in the introduction that fluids are present and play a dominant role in this region of the margin. In particular, fluid seepage has been observed at the ocean floor. When fluids are present, the related variations in pore pressure and resulting normal stresses are always involved in triggering the seismicity, whether this occurs along the plate interface or within the overriding plate. The importance of pore pressure in the generation of seismicity has been confirmed by numerous injection experiments and by drilling along a number of margins. Although we have no definite proof that this applies also to the part of the margin imaged in our data set, it would seem absurd to assume fluids play no role in this margin, in which outstandingly large amounts of fluids are available, as has been imaged by active seismic (DeShon and Schwartz 2004; Grevemeyer et al. 2007; Ivandic et al. 2008, 2010) and local earthquake tomography (Dinc et al. 2011).

The uncertainty in the absolute depth location of our events is of the order of 10 %. Therefore, we can assume that the swarm in December 2005 occurred in the down-going plate while the swarm in January 2006 happened in the overriding plate. Both swarms show a uniform P -waveform indicating a uniform fault mechanism. This means that in either case single faults became activated during the swarm. In case of the December 2005 swarm, it

could be a bending-related serpentinized fault (Ivandić et al. 2008). The January 2006 swarm occurred along a fault within the continental margin such as identified on seismic reflection profile nearby and suggested to form pathways for the vent sites. Only the March 2006 swarm took place near the plate interface covering a larger volume and showing incoherent waveforms of the *P*-phase. This indicates that the stress release occurs in a fractured volume rather than on a slip plane. The volume fracturing as such could be related to the subduction of a seamount or other topographic features. However, for the reasons discussed above, the temporal seismicity clustering would be preferably attributed to fluids released near the interface as it was proposed by Brown et al. (2005).

Observed diffusivity and permeability

If we accept that the swarms are related to fluid pressure migration, we can assess their temporal development to estimate of the diffusion constant and hydraulic permeability in the continental slope.

The range of values found for the diffusivity (28–921 m²/s) is larger than what is usually observed in borehole injection measurements (0.01 to a few m²/s) by about two orders of magnitude (Shapiro et al. 1997, 1999, 2002, 2006; Huenges and Zimmermann 1999; Rothert et al. 2003). However, the KTB drill hole, which reached 9 km depth, sampled crystalline continental crust subjected to the regional Alpine stress field. This regime, and the forced migration of injection fluids, can be expected to have lower diffusivities than natural fluid migration through a water-saturated margin wedge actively deformed by the subduction process. Based on the Antofagasta 1995 earthquake aftershock sequence, Shapiro et al. (2003) obtain a diffusivity of 200 m²/s, somewhat higher but similar to our results.

The permeability values obtained from the diffusivity are also comparatively large, ranging between 3.2×10^{-14} m² and 106.0×10^{-14} m². For a basaltic composition, this permeability is much higher than what is usually observed in laboratory experiments (of the order of 10^{-18} m² in this pressure and temperature range), but falls into the large range of values that have been estimated for the upper oceanic crust by indirect methods (for a comparative overview, see Fisher 1998, and Townend and Zoback 2000). Permeability values easily vary over several orders of magnitudes even within short lateral and vertical distances; e.g. Saffer et al. (2000) observe permeabilities between 10^{-18} and 10^{-14} m² for depths down to 5 km in drill logs on the margin wedge off north Costa Rica. An end member of high permeability is open fracture systems of near surface crystalline rock which can reach permeability values

of the order of 10^{-11} – 10^{-12} m² (e.g. Li et al. 1994). Waldhauser et al. (2012) find permeabilities of the order of 10^{-10} – 10^{-13} m² for fluid driven aftershocks of the 2004 M9.2 Sumatra–Andaman earthquake. Our estimated permeability value of $k = 3.2 \times 10^{-14}$ m²– 106.0×10^{-14} m² is comparable to the one obtained by Shapiro et al. (2003) for the Antofagasta aftershocks. The Antofagasta aftershocks occurred along the seismogenic zone, whereas from our fluid migration swarms are located above and trenchward of the seismogenic zone, where more fluids are assumed to be present. However, the comparison indicates that our estimated values are reasonable and reflect the large amount of fluids present and extensive fracturing of the margin wedge in this actively venting region.

Conclusions

On a temporary marine seismic network offshore south Nicaragua and north Costa Rica, several swarms of earthquakes are observed on the continental slope trenchward of the seismogenic zone. These swarms are relocalized by double-difference localisation and are found in the down-going slab, near the interface and in the overriding plate.

The observed swarm seismicity interpreted as an expression of pore pressure migration is used to estimate the diffusivity and permeability of the margin wedge. The swarms give consistent diffusivity values of the order of 28–305 m²/s. While these are larger than observed values from injection studies in continental boreholes, they are of comparable magnitude to values estimated for the Antofagasta 1995 earthquake aftershock sequence (Shapiro et al. 2003). The resulting permeability is about 3.2×10^{-14} m²– 35.1×10^{-14} m², based on the assumption (from Walther et al. 2000) that the margin wedge in this area is formed by subducted oceanic flood basalt. While generally high for basaltic crust, this value is similar to the one of the Antofagasta aftershocks within less than one order of magnitude. Since the swarms occur in the region along the margin wedge where fluid release by subducting sediments is greatest, we assume these values are plausible and provide an indication for extensive fracturing by fluids migrating towards the active vent sites.

Acknowledgments This publication is contribution no. 250 of the Sonderforschungsbereich 574 “Volatiles and Fluids in Subduction Zones” at Kiel University. Florian Wolf helped greatly with the data processing. We thank the ship and crew of the RV Meteor for their assistance in the deployment of the stations. For the retrieval, we are indebted to the Costa Rican coast guard, in particular, Comandante R. Peralta for providing their ship and crew for the retrieval of part of the stations. We also sincerely thank the crew of Papagayo Seafood vessel for their immense assistance with the other part of the retrieval, and for their hospitality on board.

References

- Berhorst A (2006) Die Struktur des aktiven Kontinentalhangs vor Nicaragua und Costa Rica—marin-seismische Steil- und Weitwinkelmessungen, Ph.D. thesis, Christian-Albrechts-University, Kiel
- Biot MA (1962) Mechanics of deformation and acoustic propagation in porous media. *J Appl Phys* 33:1482–1498
- Bohrmann G, Heeschen K, Jung C, Weinrebe W, Baranov B, Cailleau B, Heath R, Vühnerbach V, Hort M, Masson D, Trummer I (2002) Widespread fluid expulsion along the seafloor of the Costa Rica convergent margin. *Terra Nova* 14(2):69–79
- Brown KM, Tryon MD, DeShon HR, Dorman LM, Schwartz SY (2005) Correlated transient fluid pulsing and seismic tremor in the Costa Rica subduction zone. *Earth Planet Sci Lett* 238:189–203. doi:10.1016/j.epsl.2005.06.055
- deMets Ch, Gordon RG, Argus DF, Stein S (1994) Effects of recent revisions to the geomagnetic reversal time scale on estimates of current plate motions. *Geophys Res Lett* 31(20):2191–2194
- DeShon HR, Schwartz SY (2004) Evidence for serpentinization of the forearc mantle wedge along the Nicoya Peninsula, Costa Rica. *Geophys Res Lett* 31(L21611):4
- DeShon HR, Schwartz SY, Newman AV, González V, Protti M, Dorman LM, Dixon TH, Sampson DE, Flueh ER (2006) Seismogenic zone structure beneath the Nicoya Peninsula, Costa Rica, from three-dimensional local earthquake P- and S-wave tomography. *Geophys J Int* 164(1):109–124
- Dinc AN, Rabbel W, Flueh ER, Taylor W (2011) Mantle wedge hydration in Nicaragua from local earthquake tomography. *Geophys J Int* 186(1):99–112
- Fekete N (2006) Dewatering through mud mounds on the continental fore-arc of Costa Rica, Ph.D. thesis, Christian-Albrechts-University, Kiel
- Fisher AT (1998) Permeability within basaltic oceanic crust. *Rev Geophys* 36(2):143–182
- Gebrande H (1982) Elastic wave velocities and constants of elasticity of rocks and rock forming minerals. In: Angenheister G (ed) *Physical properties of rocks, Landolt-Börnstein numerical data and functional relationships in science and technology V1b*. Springer, Berlin, pp 1–99
- Grevemeyer I, Ranero CR, Flueh ER, Kläschen D, Bialas J (2007) Passive and active seismological study of bending-related faulting and mantle serpentinization at the Middle America trench. *Earth Planet Sci Lett* 258:528–542
- Han X, Suess E, Sahling H, Wallmann K (2004) Fluid venting activity on the Costa Rica margin: new results from authigenic carbonates. *Int J Earth Sci (Geol Rundschau)* 93:596–611
- Hensen Ch, Wallmann K, Schmidt M, Ranero CR, Suess E (2004) Fluid expulsion related to mud extrusion off Costa Rica—a window to the subducting slab. *Geology* 32(3):201–204
- Hensen C, Nuzzo M, Hornibrook E, Pinheiro LM, Bock B, Magalhães VH, Brückmann W (2007) Sources of mud volcano fluids in the Gulf of Cadiz—indications for hydrothermal imprint. *Geochim Cosmochim Acta* 71:1232–1248
- Huenges E, Zimmermann G (1999) Rock permeability and fluid pressure at the KTB. *Oil Gas Sci Technol-Rev IFP* 54(6):689–694
- Hyndman RD, Yamano M, Oleskevich DA (1997) The seismogenic zone of subduction thrust faults. *Island Arc* 6:244–260
- International Seismological Centre (2011) On-line Bulletin, <http://www.isc.ac.uk>, International Seismological Centre, Thatcham
- Ivandić M, Grevemeyer I, Berhorst A, Flueh ER, McIntosh K (2008) Impact of bending-related faulting on the seismic properties of the incoming oceanic plate offshore of Nicaragua. *J Geophys Res* 113
- Ivandić M, Grevemeyer I, Bialas J, Petersen CJ (2010) Serpentinization in the trench-outer rise region offshore of Nicaragua: constraints from seismic refraction and wide-angle data. *Geophys J Int* 180(3):1253–1264
- Kahn LM, Silver EA, Orange D, Kochevar R, McAdoo B (1996) Surficial evidence of fluid expulsion from the Costa Rica Accretionary Prism. *Geophys Res Lett* 23(8):887–890
- Karaca D, Hensen C, Wallmann K (2010) Controls on authigenic carbonate precipitation at cold seeps along the convergent margin off Costa Rica. *Geochem Geophys Geosyst* 11:Q08S27
- Klaucke I, Masson DG, Petersen CJ, Weinrebe W, Ranero CR (2008) Multifrequency geoacoustic imaging of fluid escape structures offshore Costa Rica: Implications for the quantification of seep processes. *Geochem Geophys Geosyst* 9
- Li YD, Rabbel W, Wang R (1994) Investigation of permeable fracture zones by tube-wave analysis. *Geophys J Int* 116:739–753
- Mau S, Sahling H, Rehder G, Suess E, Linke P, Soeding E (2006) Estimates of methane output from mud extrusions at the erosive convergent margin off Costa Rica. *Mar Geol* 225(1–4):129–144
- Moerz T, Fekete N, Kopf A, Brueckmann W, Kreiter S, Huehnerbach V et al (2005) Styles and productivity of mud diapirism along the Middle American margin, part II. Mound Culebra and Mounds 11 and 12. In: *Mud volcanoes, geodynamics and seismicity, NATO science series: IV: earth and environmental sciences*, vol 51, chap 1, pp 49–76
- Oleskevich DA, Hyndman RD, Wang K (1999) The updip and downdip limits to great subduction earthquakes: thermal and structural models of Cascadia, south Alaska, SW Japan and Chile. *J Geophys Res* 104:14965–14991
- Petersen CJ, Klaucke I, Weinrebe W, Ranero CR (2009) Fluid seepage and mound formation offshore Costa Rica revealed by deep-towed sidescan sonar and sub-bottom profiler data. *Mar Geol* 266(1–4):172–181
- Ranero C, von Huene R (2000) Subduction erosion along the Middle America convergent margin. *Nature* 404:748–752
- Ranero CR, Villaseñor A, Phipps Morgan J, Weinrebe W (2005) Relationship between bend-faulting at trenches and intermediate-depth seismicity. *Geochem Geophys Geosys* 6(12)
- Ranero C, Vannucchi P, von Huene R (2007) Drilling the seismogenic zone of an Erosional convergent margin: IODP Costa Rica Seismogenesis project CRISP, in: abstracts and reports from the IODP/ICDP workshop on fault zone drilling. In: Ito H, Behrmann JH, Hickman S, Tobin H, Kimura G (eds.) *Scientific drilling: special issue*, no. 1, pp 51–54
- Ranero CR, Grevemeyer I, Sahling H, Barckhausen U, Hensen Ch, Wallmann K, Weinrebe W, Vannucchi P, von Huene R, McIntosh K (2008) Hydrogeological system of erosional convergent margins and its influence on tectonics and interpolate seismogenesis. *Geochem Geophys Geosys* 9:3. doi:10.1029/2007GC001679
- Rothert E, Shapiro SA, Buske S, Bohnhoff M (2003) Mutual relationship between microseismicity and seismic reflectivity: case study at the German Continental deep drilling site (KTB). *Geophys Res Lett* 30(17):1893
- Rüpke LH, Phipps Morgan J, Hort M, Connolly JAD (2002) Are the regional variations in Central American arc lavas due to differing basaltic versus peridotitic slab sources of fluids? *Geology* 30(11):1035–1038
- Rüpke LH, Phipps Morgan J, Hort M, Connolly JAD (2004) Serpentine and the subduction zone water cycle. *Earth Planet Sci Lett* 223:17–34. doi:10.1016/j.epsl.2004.04.018
- Saffer DM, Tobin HJ (2011) Hydrogeology and Mechanics of Subduction Zone Forearcs: fluid flow and pore pressure. *Annu Rev Earth Planet Sci* 39:157–186
- Saffer DM, Silver EA, Fisher AT, Tobin H, Moran K (2000) Inferred pore pressures at the Costa Rica subduction zone: implications for dewatering processes. *Earth Planet Sci Lett* 177:193–207

- Sahling H, Masson DG, Ranero CR, Hühnerbach V, Weinrebe W, Klauke I, Bürk D, Brückmann W, Suess E (2008) Fluid seepage at the continental margin offshore Costa Rica and southern Nicaragua. *Geochem Geophys Geosys* 9(Q05S05). doi:10.1029/2008GC001978
- Schmidt M, Hensen C, Mörz T, Müller C, Grevemeyer I, Wallmann K, Mau S, Kaul N (2005) Methane hydrate accumulation in “Mound 11” mud volcano, Costa Rica forearc. *Mar Geol* 216(1–2):83–100. doi:10.1016/j.margeo.2005.01.001
- Shapiro S (2000) An inversion for fluid transport properties of three-dimensionally heterogeneous rocks using microseismicity. *Geophys J Int* 143:931–936
- Shapiro SA, Huenges E, Borm G (1997) Estimating the crust permeability from fluid-injection-induced seismic emission at the KTB site. *Geophys J Int* 131:F15–F18
- Shapiro SA, Audigane P, Royer J–J (1999) Large-scale in situ permeability tensor of rocks from induced microseismicity. *Geophys J Int* 137:207–213
- Shapiro SA, Rothert E, Rath V, Rindschwentner J (2002) Characterization of fluid transport properties of reservoirs using induced microseismicity. *Geophysics* 67(1):212–220
- Shapiro SA, Patzig R, Rothert E, Rindschwentner J (2003) Triggering of seismicity by pore-pressure perturbations: permeability-related signatures of the phenomenon. *Pure Appl Geophys* 160:1051–1066
- Shapiro SA, Kummerow J, Dinske C, Asch G, Rothert E, Erzinger J, Kümpel H–H, Kind R (2006) Fluid induced seismicity guided by a continental fault: injection experiment of 2004/2005 at the German Deep Drilling Site (KTB). *Geophys Res Lett* 33:L01309
- Soeding E, Wallmann K, Suess E, Flüh E (2003) FS Meteor, cruise report M54/2-3: Caldera-Curacao: GEOMAR report 111, p 366
- Spinelli GA, Underwood MB (2004) Character of sediments entering the Costa Rica subduction zone: implications for partitioning of water along the plate interface. *Island Arc* 13:432–451
- Talukder AR, Bialas J, Klaeschen D, Buerk D, Brueckman W, Reston T, Breitzke M (2007) High-resolution, deep tow, multichannel seismic and sidescan sonar survey of the submarine mounds and associated BSR off Nicaragua pacific margin. *Mar Geol* 241(1–4):33–43
- Townend J, Zoback M (2000) How faulting keeps the crust strong. *Geology* 40:399–402
- Vannucchi P, Scholl DW, Meschede M, McDougall-Reid K (2001) Tectonic erosion and consequent collapse of the Pacific margin of Costa Rica: combined implications from ODP Leg 170, seismic offshore data, and regional geology of the Nicoya Peninsula. *Tectonics* 20(5):649–668
- Vannucchi P, Ranero CR, Galeotti S, Straub SM, Scholl DW, McDougall-Reid K (2003) Fast rates of subduction erosion along the Costa Rica Pacific margin: implications for nonsteady rates of crustal recycling at subduction zones. *J Geophys Res* 108(B11)
- von Huene R, Ranero CR, Weinrebe W, Hinz K (2000) Quaternary convergent margin tectonics of Costa Rica, segmentation of the Cocos Plate, and Central American volcanism. *Tectonics* 19(2):314–334
- Waldhauser F (2001) hypoDD—a program to compute double-difference hypocenter locations, USGS open file report 01–113
- Waldhauser F, Ellsworth WL (2000) A double-difference earthquake location algorithm: method and application to the northern Hayward fault. *Bull Seism Soc Am* 90:1353–1368
- Waldhauser F, Schaff D, Diehl T, Engdahl R (2012) Splay faults imaged by fluid-driven aftershocks of the 2004 Mw 9.2 Sumatra-Andaman earthquake. *Geology* 40:243–246
- Walther CHE, Flueh ER, Ranero CR, von Huene R, Strauch W (2000) Crustal structure across the Pacific margin of Nicaragua: evidence for ophiolitic basement and a shallow mantle sliver. *Geophys J Int* 141(3):759–777